IOP Publishing Journal of Physics A: Mathematical and Theoretical
J. Phys. A: Math. Theor **53** (2020) 185204 (19pp) https://doi.org/10.1088/1751-8121/ab7df7

Thermodynamics of quantum phase transitions of a Dirac oscillator in a homogenous magnetic field

A M Frassino[1], D Marinelli[2], O Panella[3,6] and P Roy[4,5]

[1] Departament de Física Quàntica i Astrofísica, Institut de Ciències del Cosmos, Universitat de Barcelona, Martí i Franquès 1, E-08028 Barcelona, Spain
[2] Machine Learning and Optimization Lab., RIST, 400487 Cluj-Napoca, Romania
[3] Istituto Nazionale di Fisica Nucleare, Sezione di Perugia, Via A. Pascoli, I-06123 Perugia, Italy
[4] Atomic Molecular and Optical Physics Research Group, Advanced Institute of Materials Science, Ton Duc Thang University, Ho Chi Minh City, Vietnam
[5] Faculty of Applied Sciences, Ton Duc Thang University, Ho Chi Minh City, Vietnam

E-mail: antoniam.frassino@icc.ub.edu, dm@financial-networks.eu, orlando.panella@pg.infn.it and pinaki.roy@tdtu.edu.vn

Received 22 November 2019, revised 5 March 2020
Accepted for publication 9 March 2020
Published 15 April 2020

Abstract

The Dirac oscillator in a homogeneous magnetic field exhibits a chirality phase transition at a particular (critical) value of the magnetic field. Recently, this system has also been shown to be exactly solvable in the context of noncommutative quantum mechanics featuring the interesting phenomenon of re-entrant phase transitions. In this work we provide a detailed study of the thermodynamics of such quantum phase transitions (both in the standard and in the noncommutative case) within the Maxwell–Boltzmann statistics pointing out that the magnetization has discontinuities at critical values of the magnetic field even at finite temperatures.

Keywords: Dirac oscillator, quantum phase transition, non commutativity, reentrant quantum phase transitions

(Some figures may appear in colour only in the online journal)

[6] Author to whom any correspondence should be addressed.

1. Introduction

Quantum phase transitions (QPT) [1] are a class of phase transitions that can take place at zero temperature when the quantum fluctuations, required by the Heisenberg's uncertainty principle, cause an abrupt change in the phase of the system. The QPTs occur at a critical value of some parameters of the system such as pressure or magnetic field. In a QPT, the change is driven by the modification of particular couplings that characterise the interactions between the microscopic elements of the system and the dynamics of its phase near the quantum critical point.

For a quantum system at finite temperature T, both the thermal and the quantum fluctuations are present. The interplay between the quantum and the thermal fluctuations can either smooth out the differences between the phases (namely, no phase transition occurs at finite temperature) or there can be regimes in which some discontinuities hold, and a phase transition appears. Eventually, the thermal fluctuations prevail [1].

In this paper we shall be considering an exactly solvable relativistic system, namely the Dirac oscillator [2]. The Dirac oscillator has a lot of applications in different fields e.g., Jaynes–Cummings model and the anti Jaynes–Cummings model both of which are two level systems are related to the Dirac oscillator [3] and the noncommutative Dirac oscillator respectively [4–6]. It may also be noted that an experimental realization of the mapping of commutative Dirac oscillator to the Janynes–Cummings model has been proposed in reference [3, 7, 8]. In particular, we focus on the Dirac oscillator, at finite temperature T and with an additional constant magnetic field $\mathbf{B}$. The Dirac oscillator system including an interaction in the form of a homogeneous magnetic field is an exactly solvable system [3, 4, 9–11] and shows interesting properties. In particular, at zero temperature, if the magnitude of the magnetic field either exceeds or is less than a critical value $B_{\rm cr}$ (which depends on the oscillator strength), this combined system shows a *chirality phase transition* [12, 13]. Because of the phase transition, the energy spectrum is different for $B > B_{\rm cr}$ and $B < B_{\rm cr}$ where B is the magnetic field strength.

The $(2+1)$-dimensional Dirac oscillator in the presence of a constant magnetic field has also been studied at zero temperature in the framework of noncommutative space coordinates and momenta [14]. A remarkable feature of this system comes from the fact that at zero temperature it manifests a re-entrant phase transition (RPT) [14, 15] that we find is present also at finite temperature (see figure 1). The RPT was first observed in nicotine/water mixture [16] as noted in [17]. This phenomenon has been recently found also in gravitational systems [18, 19], and for the first time in noncommutative systems in [14, 15]. As pointed out in [20–23], there are systems in condensed matter physics that in certain regimes appear to have a behavior mathematically equivalent to systems living in a noncommutative spacetime. This opens the avenue of an *analogue noncommutativity* that is the possibility of studying, also experimentally, condensed matter systems that are analogue to those with noncommuting coordinates and/or momenta but living in ordinary commutative space.

Indeed, it has been shown in [10] that in the $(2+1)$-dimensional Dirac oscillator $B_{\rm cr}$ depends not only on the oscillator strength but also on the noncommutative parameters. The consequence of the noncommutative scenario is that, apart from the left- and right-chiral phases of the commutative case, there is also a third left phase and thus a second quantum phase transition (right-left) [14] (see figure 1). The presence of this third phase with left chirality leads to the RPT [15].

In this work, we analyze the Dirac oscillator in the presence of a constant magnetic field at finite temperature. While in the first part of the paper we consider the thermodynamics of the standard system the second part will be dedicated to the thermodynamics of the noncommutative Dirac oscillator.

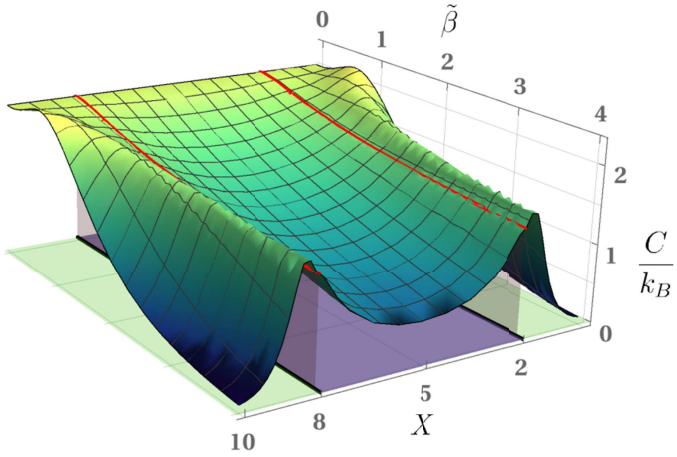

Figure 1. Re-entrant phase transition as shown by the heat capacity of a noncommutative Dirac oscillator as a function of the scaled effective magnetic energy $X \equiv (\mu B - \hbar\omega)/mc^2$ and the scaled inverse temperature $\tilde{\beta} = mc^2/k_B T$. The two critical (red) lines $X_1 = \omega_\eta \hbar/mc^2 = 2$ and $X_2 = \left(\omega_\theta \hbar/mc^2\right) = 8$ divide the green regions (left phases) from the violet region (right phase). In the left phases, the heat capacity becomes non-monotonic in $\tilde{\beta}$.

To study what kind of QPT the Dirac oscillator at finite T undergoes, we will investigate the system at high temperatures when the statistics can be approximated with the Maxwell–Boltzmann one [24]. We find that in this regime the QPT does not disappear and therefore the quantum fluctuations prevail upon the thermal ones (as can be seen in the noncommutative case in figure 1). Only in the limit of very high temperatures ($\beta \to 0$) the QPT disappears.

The organization of the paper is as follows: in section 2 we shall present the system to be analyzed and discuss the spectrum of the two phases, namely, the left and the right phase; in section 3, we present the method to calculate the partition function that characterizes the chiral phases at finite temperature and describes the phase transition as the strength of the magnetic field varies; in section 4 we scrutinize in details the magnetization at finite temperature and in section 6 we study the thermodynamic of a noncommutative Dirac oscillator with a constant magnetic field. Finally, section 7 is devoted to conclusions.

2. The quantum system: Dirac oscillator with a constant magnetic field

The non-relativistic version of the $(2+1)$-dimensional Dirac oscillator with a constant magnetic field and zero temperature can be associated to a chiral harmonic oscillator [12], that have been studied in [25]. Moreover, in [26, 27] a possible connection to topological Chern–Simons gauge theories has been pointed out. The case of the system presented in this paper can be seen as a relativistic extension of the chiral harmonic oscillators [12, 13], at finite temperature.

A relativistic spin-1/2 fermion constrained in a two-dimensional plane with mass m, charge e, Dirac oscillator frequency ω and subjected to an a constant magnetic field orthogonal to the plane, is described by the Hamiltonian:

$$H = c\,\boldsymbol{\sigma} \cdot \left(\boldsymbol{p} - \mathrm{i}m\omega\sigma_z \boldsymbol{x} + \frac{e}{c}\boldsymbol{A}\right) + \sigma_z\, mc^2, \tag{1}$$

where c stands for the speed of light and $\boldsymbol{\sigma} = \left(\sigma_x, \sigma_y\right)$, σ_z denotes the Pauli matrices. As in the usual notation, the $\boldsymbol{p}$ and the $\boldsymbol{x}$ represent the momentum and the position operators while the vector potential is related to the magnetic field through

$$\boldsymbol{A} = (-By/2, Bx/2). \tag{2}$$

The relativistic oscillator interaction acts as an effective transverse magnetic field. This set-up offers an intriguing interplay: while the two-dimensional Dirac oscillator coupling endows the particle with an intrinsic left-handed chirality [3], the magnetic field coupling favors a right-handed chirality [9]. The interplay between opposed chirality interactions culminates in the appearance of a relativistic quantum phase transition, which can be fully characterized [12].

2.1. Energy levels

In this section, we shall recall the spectrum [3, 4, 9–13] and the degeneracy of the various energy levels of a two-dimensional relativistic Dirac oscillator in the two phases defined by $B > B_{\rm cr}$ and $B < B_{\rm cr}$. The spectrum of the system is characterized by two quantum numbers: $n_{\rm r} = 0, 1, 2, \ldots$, the radial quantum number and $M = 0, \pm 1, \pm 2, \ldots$, the two-dimensional angular momentum quantum number (please refer to [14] for the detailed analysis of the spectrum).

In what we call the *left phase*, the energy level corresponding to the zero mode has positive energy $E = mc^2$ and infinite degeneracy with respect to the non-negative magnetic quantum number $M \geqslant 0$ (the negative magnetic numbers are forbidden [14], but only for the zero mode).

The excited states, which contain both positive and negative M, are

$$E_N^{\pm} = \pm mc^2 \sqrt{1 + \xi_{\rm L} N}, \tag{3}$$

$$N = n_{\rm r} + \frac{|M| - M}{2}, \quad N = 1, 2, \ldots, \tag{4}$$

where N labels the energy levels, $\xi_{\rm L}$ is a constant encoding the parameters of the system that for the standard commutative case simply reads

$$\xi_{\rm L} = -4\,X, \quad X := \frac{1}{mc^2}\left(\mu B - \hbar\omega\right) \tag{5}$$

and $\mu = e\hbar/(2mc)$ denotes the Bohr magneton. The energy levels in (4) are degenerate. In particular, every level has infinite degeneracy, with respect to the non-negative values of M, and $D = N + 1$ finite degeneracy with respect to the negative values of M.

The *right phase*, on the other hand, has zero mode degeneracy with respect to the non-positive magnetic quantum number $M \leqslant 0$ and the value of the energy is in the negative branch: $E = -mc^2$. Similarly, the excited states have an infinite degeneracy with respect to non-positive values of M, while the degeneracy is $D = N + 1$ with respect to $M > 0$ and the energies read

$$E_N^{\pm} = \pm mc^2 \sqrt{1 + \xi_{\rm R} N}, \quad N = n_{\rm r} + \frac{|M| + M}{2} \quad N = 1, 2, \ldots, \tag{6}$$

where the parameter $\xi_{\rm R}$ is related to $\xi_{\rm L}$ by the relation $\xi_{\rm R} = -\xi_{\rm L}$. Note that, when $\xi_{\rm R} = \xi_{\rm L} = 0$, that is when

$$B = B_{\rm cr} = \hbar\,\mu\,\omega, \tag{7}$$

all the energy levels collapse to the energy $E = \pm mc^2$ and the *quantum phase transition* happens [12, 14].

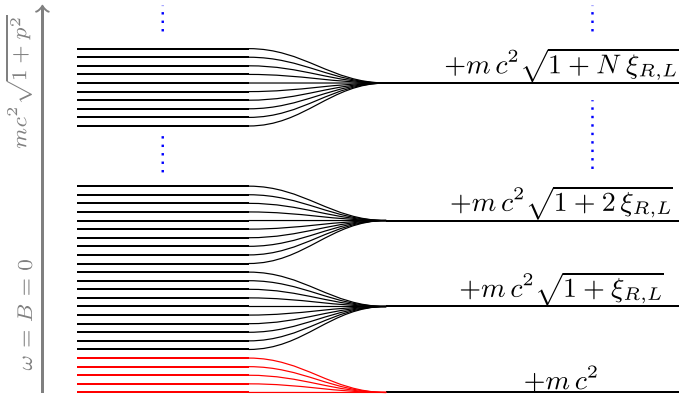

Figure 2. Pictorial view of the positive branch of the energy levels that from a continuous spectrum for the free electron collapse to the discrete one in (4) and (6).

3. Finite temperature quantum phase transition

To study the interplay between thermal and quantum fluctuations for this two-dimensional relativistic Dirac oscillator, we focus on the system at high temperatures when the electron-states statistics can be described with the Maxwell–Boltzmann statistics. We will show that in this regime the QPT will not disappear.

3.1. Partition function

The partition function for the positive branch of the energy levels (4) and (6) and the zero mode, has to take into account the degeneracy of each single energy level. Thus, it is defined by the product of the density of the states and the Boltzmann factor

$$Z_{\mathrm{L,R}} = \sum_{M,n_{\mathrm{r}}} \mathsf{g}\, \mathrm{e}^{-\beta\, E_N^+}, \quad N = 0, 1, \ldots, \tag{8}$$

where E_N^+ are the values given by (4) and (6), and β is the inverse temperature.

To evaluate the density of the states g, we can split every chiral phase of the system (left and right introduced in the previous section) into two different sub-systems with respect to the sign of the quantum number M.

If we consider a free electron with $M > 0$ or alternatively $M < 0$, in a standard commutative spacetime and confined to a finite area L^2, the number of energy levels in the region $\mathrm{d}p_x\mathrm{d}p_y$ around p_x and p_y is $\mathrm{d}\mathsf{g} = \mathsf{L}^2/\left(2h^2\right)\mathrm{d}p_x\mathrm{d}p_y$ [24]. Note that it can be proved that the phase-space volume element $\mathrm{d}p_x \wedge \mathrm{d}p_y$ in the relativistic case is invariant for Lorentz transformations [28]. Moreover, L is the length in a rest-frame.

3.1.1. Left Phase. For $M \geqslant 0$, the degeneracy of each energy level (4) defined in the region $\mathscr{K}$ of the momenta (p_x, p_y) such that $E_N < E_{\mathrm{free}}(p_x, p_y) < E_{N+1}$ (see figure 2), where E_{free} is the energy of the free electron, is given by

$$\begin{aligned} g_{M>0} &= \frac{1}{2}\left(\frac{\mathsf{L}}{h}\right)^2 \iint_{\mathscr{K}} \mathrm{d}p_x\mathrm{d}p_y \\ &= \pi\left(\frac{\mathsf{L}}{h}\right)^2 \left[p^2\right]_{\frac{p^2}{m^2c^2}=\xi_{\mathrm{L}}N}^{\frac{p^2}{m^2c^2}=\xi_{\mathrm{L}}(N+1)} = \left(\frac{\mathsf{L}mc}{h}\right)^2 \pi\xi_{\mathrm{L}}. \end{aligned} \tag{9}$$

and N depends only on the quantum number n_{r} because the difference in (4) is zero.

In the case $M < 0$, the number of levels collapsing into the level N is still equal to $\mathsf{g}_{M>0}$. However, one should consider that, when $M < 0$, as shown in (4), N depends on both the quantum number M and n_{r}, namely $N = n_{\mathrm{r}} + M$. Therefore, one needs to keep into account, for each energy level N, the degeneracy D, i.e. $\mathsf{g}_{M<0} = \mathsf{g}_{M>0}/D$.Thus, the number of states

$$\mathsf{g}_{M<0} = \left(\frac{\mathsf{L}mc}{h}\right)^2 \frac{\pi\xi_{\mathrm{L}}}{(n_{\mathrm{r}} - M + 1)}, \tag{10}$$

is not constant along the spectrum, but depends on the energy level.

Taking into account the degeneracy, using the spectrum (4) and its zero point energy, the partition function with Boltzmann statistics of the states of a single oscillator[7] for the left phase is

$$Z_{\mathrm{L}} = \left(\frac{\mathsf{L}mc}{h}\right)^2 \pi\xi_{\mathrm{L}} \left[\mathrm{e}^{-\beta mc^2} + \sum_{n_{\mathrm{r}}=1}^{\infty} \mathrm{e}^{-\beta mc^2\sqrt{1+\xi_{\mathrm{L}}\, n_{\mathrm{r}}}} + \sum_{n_{\mathrm{r}}=1}^{\infty}\sum_{M=0}^{-\infty} \frac{\mathrm{e}^{-\beta mc^2\sqrt{1+\xi_{\mathrm{L}}\,(n_{\mathrm{r}}-M)}}}{(n_{\mathrm{r}} - M + 1)}\right]. \tag{11}$$

Notice that the contribution to the partition function of the zero mode energy appears only for $M \geqslant 0$ [14] and, as we will see later in section 3.3, this will be the source of the non-analyticity of the partition function at the phase point. The sum in the third term of (11) coincides with the second if we introduce M' and N' such that $M' = -M$ then $n_{\mathrm{r}} + M' = N'$, obtaining

$$\sum_{n_{\mathrm{r}}=1}^{\infty}\sum_{N'=n_{\mathrm{r}}}^{\infty} \frac{\mathrm{e}^{-\beta mc^2\sqrt{1+\xi_{\mathrm{L}}\,(N')}}}{(N'+1)} = \sum_{N'=1}^{\infty} \mathrm{e}^{-\beta mc^2\sqrt{1+\xi_{\mathrm{L}}\,(N')}}, \tag{12}$$

so, over all, the two sectors ($M > 0$ and $M < 0$) equally contribute to the partition function.

3.1.2. Right Phase. The partition function for the right phase, defined by the energy levels (6), is equal to (11) except for the zero mode term. This is because, as explained in section 2, the zero mode contributes only to the negative energies branch.

3.2. Zeta-function representation

A different representation of the defining series in the partition function that will reveal itself to be more effective when the phase switches from left to right, can be obtained using the Cahen–Mellin integral, as suggested for different systems in [29] and reviewed in [30, 31]. The Cahen–Mellin integral is defined as [32]

$$\mathrm{e}^{-x} = \frac{1}{2\pi\mathrm{i}}\int_{\mathfrak{c}-\mathrm{i}\infty}^{\mathfrak{c}+\mathrm{i}\infty} \Gamma(s)\, x^{-s}\, \mathrm{d}s \quad \left(|\arg x| < \frac{1}{2}\pi;\, x \neq 0\right) \tag{13}$$

where $\mathfrak{c}$ is real and $\mathfrak{c} > 0$. The argument of the integral has poles for all $x = -n, n \in \mathbb{N}_0$ and the residuals at the negative poles are $(-1)^n/n!$ (see figure 3). Using (13) to calculate the second

[7] The classical multi-oscillator states partition function is simply $(Z_{\mathrm{L}})^n/n!$ for n electrons [24].

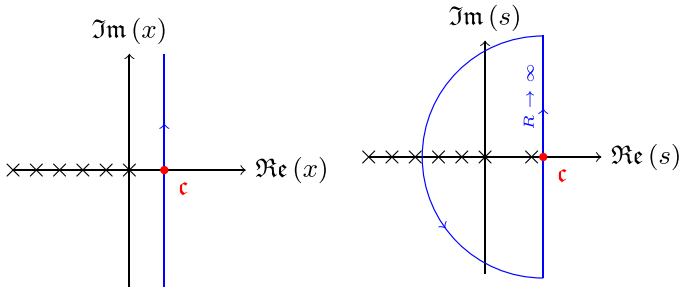

Figure 3. (Left) Poles of the argument of the Cahlen–Mellin integral (13). (Right) Path in the complex plane over which the contour integration (16) is performed. The semicircle of radius $R\to\infty$ is closed on the left.

term in the partition function (11) and including the sum into the integral, we have that the term

$$\xi_{\mathrm{L}}\sum_{n_{\mathrm{r}}=1}^{\infty}\mathrm{e}^{-\beta mc^2\sqrt{1+\xi_{\mathrm{L}}\,n_{\mathrm{r}}}} \tag{14}$$

can be rewritten as

$$\frac{\xi_{\mathrm{L}}}{2\pi\mathrm{i}}\int_{\mathfrak{c}-\mathrm{i}\infty}^{\mathfrak{c}+\mathrm{i}\infty}\frac{\Gamma(s)}{\left(\beta mc^2\right)^s}\sum_{n_{\mathrm{r}}=1}^{\infty}\frac{1}{(1+\xi_{\mathrm{L}}\,n_{\mathrm{r}})^{s/2}}\,\mathrm{d}s. \tag{15}$$

The series in (15) can be recognized as the series representation of the Hurwitz-ζ function $\zeta(v,a)=\sum_{n=0}^{\infty}\frac{1}{(n+a)^v}$ that converges only if $\mathfrak{Re}\,(v)>1$. Under this condition the integral (15) becomes

$$\frac{\xi_{\mathrm{L}}}{2\pi\mathrm{i}}\int_{\mathfrak{c}-\mathrm{i}\infty}^{\mathfrak{c}+\mathrm{i}\infty}\frac{\Gamma(s)}{\left(\beta mc^2\xi_{\mathrm{L}}^{1/2}\right)^s}\zeta\left(\frac{s}{2},\frac{1}{\xi_{\mathrm{L}}}+1\right)\,\mathrm{d}s. \tag{16}$$

In contrast to what has been proposed in the recent literature on the topic (see [31] and references therein), we notice that the condition for the convergence of the series $s/2>1$ implies $\mathfrak{c}>2$. The integral can therefore be evaluated with the method of residue once a proper closed path has been identified. Because of the presence of the Γ-function that diverges as $\Gamma(s)=(2\pi)^{1/2}\mathrm{e}^{-s}s^{s-\frac{1}{2}}\left[1-\mathcal{O}\left(s^{-1}\right)\right]$, the integration in (16) can be closed only on the left part of the complex plane, allowing to use the Cauchy's residue theorem on the poles $\{s=2,0,\mathbb{Z}^-\}$ represented in figure 3. Introducing the adimensional variable $\tilde{\beta}=\beta m\,c^2$, the partition functions for both the phases becomes

$$\begin{aligned}Z_{\mathrm{L,R}}=2\pi\left(\frac{\mathsf{L}mc}{h}\right)^2\Bigg[&\left(\frac{2}{\tilde{\beta}^2}-1\right)+\left(\frac{\Theta\mathrm{e}^{-\tilde{\beta}}}{2}-\frac{1}{2}\right)\xi_{\mathrm{L,R}}\\&+\sum_{n=1}^{\infty}\frac{\left(-\tilde{\beta}\right)^n\xi_{\mathrm{L,R}}^{\frac{n}{2}+1}}{n!}\zeta\left(-\frac{n}{2},1+\frac{1}{\xi_{\mathrm{L,R}}}\right)\Bigg],\end{aligned} \tag{17}$$

where now we use the subscript L, R to indicate both the left and right phase and Θ is a step function that is equal to zero (one) for the right phase (left phase). This series representation

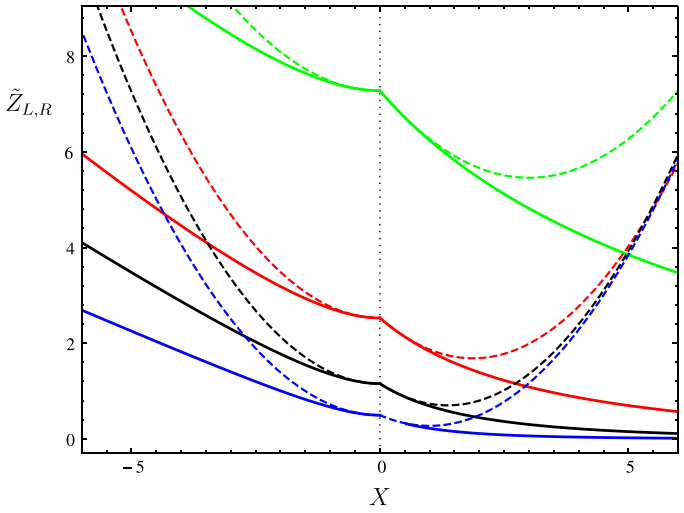

Figure 4. Scaled partition function for the commutative Dirac oscillator and its second order approximation at the critical point (dashed) as a function of the scaled effective magnetic energy X, defined in (5), for different values of the temperature: $\tilde{\beta} = 0.5,\ 0.8,\ 1.1,\ 1.5$ respectively green, red, black and blue lines.

can be seen as a series expansion in power of β, namely a high-temperature power expansion. From now on the quantity in the square brackets of (17) will be called $\tilde{Z}_{\mathrm{L,R}}$

$$Z_{\mathrm{L,R}} = 2\pi\left(\frac{\mathsf{L}mc}{h}\right)^2 \tilde{Z}_{\mathrm{L,R}}. \tag{18}$$

The series representations of the partition function $\tilde{Z}_{\mathrm{L,R}}$ in terms of the ζ-function and the Boltzmann representation introduced in (11) can be both evaluated numerically considering only a finite number of terms in the series. However, the Boltzmann representation encounters obvious numerical issues for small values of $\xi_{\mathrm{L,R}}$, i.e. close to the value where the phase transition happens. These issues do not affect the ζ-function representation of the partition function and, as we will see in the next subsection, the partition function can be evaluated analytically for small values of $\xi_{\mathrm{L,R}}$. Figure 4 shows $\tilde{Z}_{\mathrm{L,R}}$ in the ζ-function representation keeping $n_{\max} = 100$ terms of the series in (17).

3.3. Partition function near the critical point

The partition function (17) can be used to calculate the asymptotic expansion near the critical point, namely when $\xi_{\mathrm{L,R}} \to 0$. This allows to analytically explore the regimes close to the phase transition and study the interplay between thermal and quantum fluctuations. The asymptotic expansion of the Hurwitz-ζ function [33, 34] is

$$\zeta(s,a) = \frac{a^{1-s}}{s-1} + \frac{1}{2}a^{-s} + \frac{\mathsf{Z}(s,a)}{\Gamma(s)} \tag{19}$$

where the large-a (Poincaré) asymptotic expansion of the function $\mathsf{Z}(s,a)$

$$\mathsf{Z}(s,a) \sim \sum_{k=1}^{\infty} \frac{B_{2k}}{(2k)!} \frac{\Gamma(2k+s-1)}{a^{2k+s-1}}, \quad |a| \to \infty \tag{20}$$

is valid in $|\arg a| < \pi$ and B_{2k} denote the even-order Bernoulli numbers. Writing explicitly the sum (20) in the partition function $\tilde{Z}_{\mathrm{L,R}}$ gives

$$\begin{aligned}\tilde{Z}_{\mathrm{L,R}} = \frac{2}{\tilde{\beta}^2} - 1 - \left(1 - \Theta \mathrm{e}^{-\tilde{\beta}}\right) \frac{\xi_{\mathrm{L,R}}}{2} \\ + \sum_{n=1}^{\infty} \frac{\left(-\tilde{\beta}\right)^n}{n!} \left\{ \left[\frac{1}{2}\xi_{\mathrm{L,R}} - \frac{2\left(\xi_{\mathrm{L,R}}+1\right)}{n+2} \right] \left(\xi_{\mathrm{L,R}}+1\right)^{\frac{n}{2}} \right. \\ \left. + \sum_{k=1}^{\infty} \frac{B_{2k}}{(2k)!} \frac{\Gamma\left(2k - \frac{n}{2} - 1\right)}{\Gamma\left(-\frac{n}{2}\right)} \frac{\xi_{\mathrm{L,R}}^{2k}}{\left(\xi_{\mathrm{L,R}}+1\right)^{2k-\frac{n}{2}-1}} \right\}. \end{aligned} \tag{21}$$

Using the binomial series and the relation between Euler gamma functions

$$\Gamma\left(-\frac{n}{2}\right) \Gamma\left(1+\frac{n}{2}\right) = \frac{\pi}{\sin\left(-\pi n/2\right)}, \tag{22}$$

one can rewrite the terms in the curly brackets in (21) as

$$\sum_{w=0}^{\infty} \frac{1}{w!} \left\{ \left[\frac{1}{2}\xi_{\mathrm{L,R}} - \frac{2\left(\xi_{\mathrm{L,R}}+1\right)}{n+2} \right] \frac{\Gamma\left(1+\frac{n}{2}\right)}{\Gamma\left(1+\frac{n}{2}-w\right)} \xi_{\mathrm{L,R}}^{w} + \sum_{k=1}^{\infty} \frac{B_{2k}}{(2k)!} \frac{\Gamma\left(1+\frac{n}{2}\right)}{\Gamma\left(-2k+\frac{n}{2}+2-w\right)} \xi_{\mathrm{L,R}}^{2k+w} \right\} \tag{23}$$

defining in this way the partition function at all orders in $\xi_{\mathrm{L,R}}$ near the critical point. At the second order in $\xi_{\mathrm{L,R}}$, one can sum the partition function at all orders in β, so that, near the critical point, it reads

$$\tilde{Z}_{\mathrm{L,R}} = \frac{2\mathrm{e}^{-\tilde{\beta}}}{\tilde{\beta}} \left[1 + \frac{1}{\tilde{\beta}} + (\Theta - 1) \frac{\tilde{\beta}\xi_{\mathrm{L,R}}}{4} + \frac{\tilde{\beta}^2 \xi_{\mathrm{L,R}}^2}{48} \right] + \mathcal{O}\left(\xi_{\mathrm{L,R}}^3\right). \tag{24}$$

This expression is a continuous but non-analytic function in $\xi_{\mathrm{L,R}}$ and, in fact, Θ brings a discontinuity in the first order derivatives. The function to the second order (24) is compared with (17) in figure 4.

4. Magnetization at finite temperature

At this point, it is possible to use the derived expression for the partition function (17) to calculate a physical observable quantity like the magnetization [35, 36]. Indeed, in [14] the magnetization has been proposed as the quantity able to distinguish between the phases of the system.

The magnetization for a system at finite temperature, can be defined as [24]

$$M = k_{\mathrm{B}} T \frac{\partial \log Z}{\partial B} = \frac{1}{\beta Z} \frac{\partial Z}{\partial \xi} \frac{\partial \xi}{\partial X} \frac{\partial X}{\partial B}. \tag{25}$$

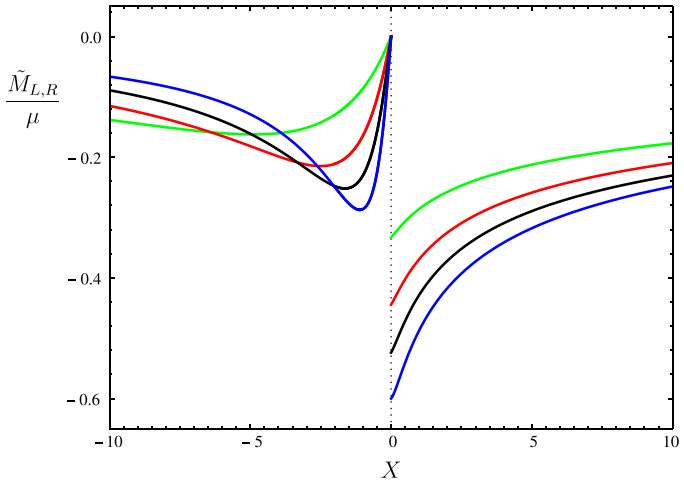

Figure 5. Scaled magnetization of the commutative Dirac oscillator as function of the scaled effective magnetic energy X, defined in (5), for different values of the temperature $\tilde{\beta} = 0.5,\ 0.8,\ 1.1,\ 1.5$ respectively green, red, black and blue lines.

In order evaluate the derivative $\partial Z/\partial \xi_{\mathrm{L,R}}$ one can use in (17) the following identity [37]

$$\frac{\partial \zeta(s,a)}{\partial a} = -s\zeta(s+1,a) \ \text{ for } s \neq 0, 1\ \mathfrak{Re}\ a > 0. \tag{26}$$

The magnetization evaluated numerically with $n_{\max} = 60$ is illustrated in figure 5. Interestingly, we find that the magnetization in the left phase, has opposite sign with respect to the single state result obtained at $T = 0$ [14]. At finite temperature, in $\xi_{\mathrm{L}} = \xi_{\mathrm{R}} = 0$ the magnetization manifests a discontinuity.

Analogously to what has been done for the partition function in the previous sections, we now inspect the magnetization behavior at values of the magnetic field close to the critical values. To approximate the full partition function in the neighborhood of $\xi_{\mathrm{L}} = \xi_{\mathrm{R}} = 0$, we can either follow the steps described in section 3.3 for the full partition function resulting of (25), or we can use (24) in (25).

At the critical point, the magnetization is not a continuous function of the magnetic field and can be written as a series expansion around $X = 0$ at all order in β as

$$\frac{M_{\mathrm{R,L}}}{\mu} = -\frac{\tilde{\beta}}{\tilde{\beta}+1} H(X) + \left(\frac{\tilde{\beta}}{\tilde{\beta}+1}\right)^2 \left[\frac{2}{3} + \tilde{\beta}\left(H(-X) - \frac{1}{3}\right)\right] X + \mathcal{O}\left(X^2\right), \tag{27}$$

where $H(x)$ is the Heaviside step function. The discontinuity with respect to the magnetic field at the critical point $X = 0$ is

$$|\Delta M_{\mathrm{cr}}| = \mu \frac{\tilde{\beta}}{(1+\tilde{\beta})}. \tag{28}$$

In the limit $\tilde{\beta} \to 0$, the thermal fluctuations overcome the quantum ones, the gap disappears and the magnetization is zero for both the chiralities.

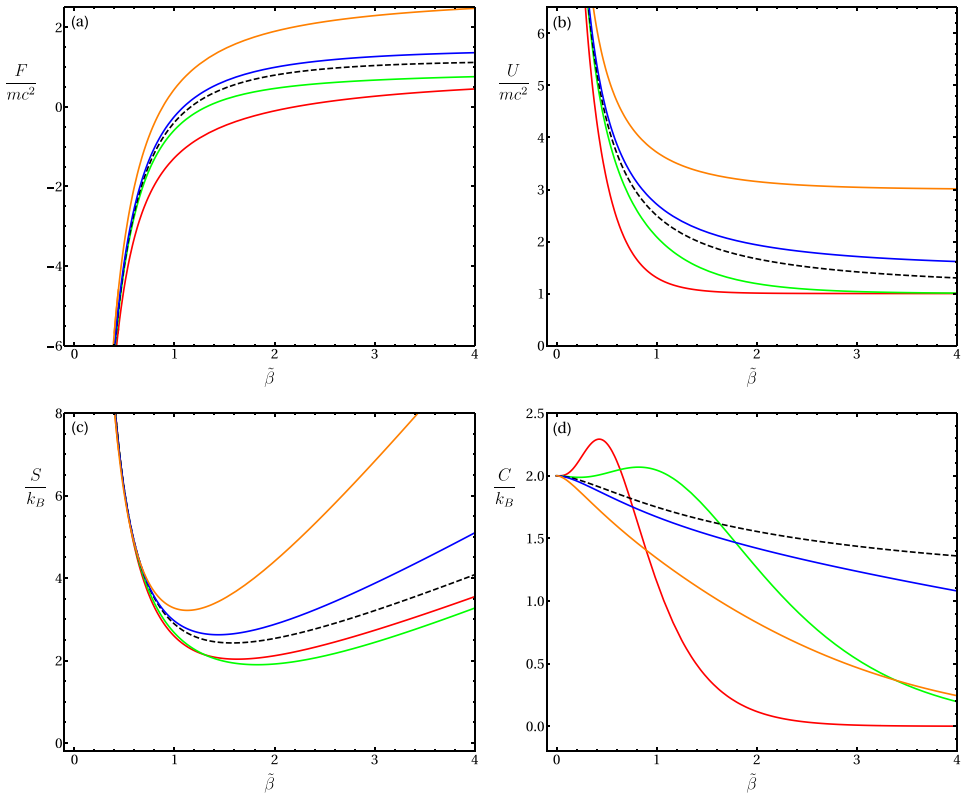

Figure 6. Various thermodynamic functions versus the scaled inverse temperature $\tilde{\beta} = mc^2/k_{\rm B}T$ for different values of the magnetic field, corresponding to $X = -4.5, -1.3, 0, 0.3, 2$ respectively red, green, dashed-black, blue, orange. The $X = 0$ case (dashed black) represents the critical value of the magnetic field. Upper left panel (a): the free energy F/mc^2; upper right panel (b): the internal energy U/mc^2; lower left (c): the entropy $S/k_{\rm B}$ and finally in the lower right panel (d) the specific heat $C/k_{\rm B}$. In the last one, it is visible the difference between the red and green (left phase) and the blue and orange (right phase).

5. Other thermodynamic functions

Once the partition function has been calculated, the thermodynamics of the system can be fully explored. Using

$$F = -\frac{1}{\beta}\ln Z, \quad U = -\frac{\partial}{\partial\beta}\ln Z,$$
$$S = k_{\rm B}\beta^2\frac{\partial F}{\partial\beta}, \quad C = -k_{\rm B}\beta^2\frac{\partial U}{\partial\beta}, \tag{29}$$

in figure 6, we plot the thermodynamic quantities for the commutative system. The specific heat as function of the β manifests a non-monotonic behavior in the left phase, while it becomes monotonic in the right phase. We note that in the high-temperature limit, $\beta \to 0$, the system reaches the same specific heat independent of the value of the magnetic field, or the X variable related to the magnetic field by (5). We can see it exactly for small values

of X using (24): $C/k_{\mathrm{B}} = 2 + O\left(X^2\right)$. The limiting value $C/k_{\mathrm{B}} = 2$ reflects the equipartition theorem for a two-dimensional system with the two additional degrees of freedom associated with the spin of the particle [24]. In the high-temperature regime, no changes in sign of C appear, showing that there is no apparent phase transition caused by the thermal fluctuations. In the left phase, the asymptote is reached from above with respect to the critical value of X. We interpret the non-monotonicity of the specific heat in the left-phase as due to the presence of the zero-mode in the partition function. This is the only difference between the left- and right-phase partition function, cf see (11).

6. Dirac oscillator with a constant magnetic field

In the previous sections we described the Dirac oscillator under a uniform magnetic field and its associated QPT in a 2D + 1 space-time.

We now, discuss the same system (Dirac oscillator in a uniform magnetic field) in a setting, i.e. assuming that the phase-space is. It might be noted that several studies of quantum field theory in a settings have appeared in the literature. Examples of renormalizable scalar field theories (ϕ^4 models), in the four-dimensional Moyal space have been discussed in [38–40]. gauge theories on three-dimensional spaces $\mathbb{R}^3_\lambda$ (a deformation of $\mathbb{R}^3$) can be found in [41–43]. Finally quantum gravity inspired noncommutative models have been discussed in [44–47].

Several studies in quantum gravity and string theory have analyzed quantum mechanical effects due to the space-time that can be fundamentally or effectively described by a generalization of geometry where, locally, coordinates do not necessarily commute [48–58]. Moreover, recent developments in condensed matter physics, suggest the use of the noncommutative geometry framework to encode geometrical properties of topological quantum systems [20–23].

The study of the Dirac oscillator in the presence of noncommutative coordinates and momenta and a constant magnetic field in a two-dimensional space at zero-temperature has been carried out in [14]. The system that in the commutative case undergoes a quantum phase transition at finite magnetic field, also exhibits in the noncommutative case another phase transition at a higher magnetic field. The third region appears to have the same chirality of the first one providing a re-entrant quantum phase transition [15].

In this section, we will study the noncommutative system at finite temperature, the parameterization that has been used for the exact calculation of the spectrum in [14] will allow us to exploit all the calculation done in the previous sections and easily study the QPTs in the noncommutative space.

6.1. Energy levels

Following the notation in [14] in this subsection we review the energy spectrum of the noncommutative system and we highlight the differences with the commutative case. The Hamiltonian for the (2 + 1)-dimensional Dirac oscillator in the noncommutative plane with a homogeneous magnetic field can be written in a way similar to (1)

$$\hat{H} = c\boldsymbol{\sigma}.\left(\hat{\boldsymbol{p}} - \mathrm{i}m\omega\sigma_z\hat{\boldsymbol{x}} + \frac{e}{c}\hat{\boldsymbol{A}}\right) + \sigma_z mc^2, \tag{30}$$

where now the *hat* indicates the noncommutative operators. In this framework, the commutation relation between coordinates and momenta are given by [48]

$$[\hat{x}, \hat{y}] = \mathrm{i}\theta, \quad [\hat{p}_x, \hat{p}_y] = \mathrm{i}\eta, \quad [\hat{x}_i, \hat{p}_j] = \mathrm{i}\hbar\left(1 + \frac{\theta\eta}{4\hbar^2}\right)\delta_{ij}, \tag{31}$$

where $\theta, \eta \in \mathbb{R}$. The noncommuting coordinates and momenta can be expressed in terms of commuting ones using the Seiberg–Witten map and are given by

$$\begin{aligned} \hat{x} &= x - \frac{\theta}{2\hbar} p_y, \quad \hat{p}_x = p_x + \frac{\eta}{2\hbar} y, \\ \hat{y} &= y + \frac{\theta}{2\hbar} p_x, \quad \hat{p}_y = p_y - \frac{\eta}{2\hbar} x. \end{aligned} \tag{32}$$

The Hamiltonian (30) can be rewritten as

$$H = c \begin{pmatrix} mc & \hat{\Pi}_- \\ \hat{\Pi}_+ & -mc \end{pmatrix}, \tag{33}$$

where $\hat{\Pi}_\pm$ are given by

$$\hat{\Pi}_\pm = \left(1 - \frac{\tilde{\omega} - \omega}{\omega_\theta}\right)(p_x \pm \mathrm{i}\, p_y) \pm \mathrm{i}\, m\, (\tilde{\omega} - \omega - \omega_\eta)(x \pm \mathrm{i} y) \tag{34}$$

after introducing the following frequencies out of the parameters of the system:

$$\tilde{\omega} = \frac{eB}{2mc}, \qquad \omega_\theta = \frac{2\,\hbar}{m\theta}, \qquad \omega_\eta = \frac{\eta}{2\hbar m}. \tag{35}$$

With this parameterization it is clear that there are two critical values of the magnetic field

$$B_{\mathrm{cr}} = \frac{2mc}{e}(\omega + \omega_\eta) = \frac{2c}{e}\left(m\omega + \frac{2\eta}{\hbar}\right), \tag{36}$$

$$B^*_{\mathrm{cr}} = \frac{2mc}{e}(\omega + \omega_\theta) = \frac{2c}{e}\left(m\omega + \frac{\hbar}{\theta}\right). \tag{37}$$

such that for both $B = B_{\mathrm{cr}}$ and $B = B^*_{\mathrm{cr}}$, there are no interactions in the model and the Hamiltonian represents a free particle (only kinetic energy). Since the critical value B_{cr} depends on the momentum noncommutative parameter η, this shifts the value of the critical field relative to the value in (7). The space noncommutativity ($\theta \neq 0$) instead introduces the additional critical value for the magnetic field (B^*_{cr}) [14].

Interestingly, the parameters used in the noncommutative massive Dirac oscillator can be reabsorbed in such a way that one can study the single phases independently. In fact, the behavior of the single phases can be described regardless of the parameters encoding the noncommutative physics [14]. Therefore, although the noncommutative system has two more parameters, they can recast into the parameter $\xi_{\mathrm{L,R}}$ allowing us to use most of the calculations performed in the previous sections for the commutative case. The main difference now is that the magnetic field and the noncommutative parameters are related by

$$\xi_{\mathrm{L}} = -4\frac{mc^2}{\omega_\theta \hbar}\left(\frac{\omega_\theta \hbar}{mc^2} - X\right)\left(X - \frac{\omega_\eta \hbar}{mc^2}\right) \tag{38}$$

while it is still valid the relation $\xi_{\mathrm{R}} = -\xi_{\mathrm{L}}$. Phase changes occur at critical values of the magnetic field that makes the parameter $\xi_{\mathrm{L,R}}$ null. Note that, differently from the commutative case (5), in the noncommutative case the equation (38) is quadratic in B and consequently it admits two critical points [14].

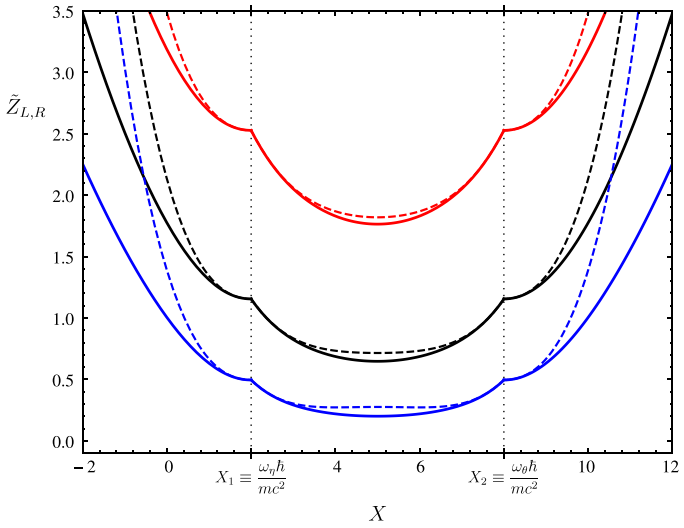

Figure 7. Scaled partition function in the noncommutative case and its approximation near the critical points X_1, X_2 (dashed) with $X_1 = \omega_\eta \hbar/mc^2 = 2$, $X_2 = \left(\omega_\theta \hbar/mc^2\right) = 8$ and $\tilde{\beta} = 0.8, 1.1, 1.5$ for respectively red, black and blue lines.

6.2. Energy levels and partition function

In section 2.1 we reviewed the spectrum of the system as a function of the parameter $\xi_{\mathrm{L,R}}$. As mentioned above, for the noncommutative case, the spectrum remains equal to (4) and (6) as a function of the parameter $\xi_{\mathrm{L,R}}$ that now becomes (38), quadratic in B. Since the density of the energy states is also a function of the parameters $\xi_{\mathrm{L,R}}$, its contribution to the partition function of each energy level in the noncommutative case coincides with the one in the commutative case (10). The resulting partition function is illustrated in figure 7. In the plot is also represented the outcome of the approximation once the constant $\xi_{\mathrm{L,R}}$ in (38) is replaced in (24). The partition function can be used to calculate the other thermodynamic quantities using (29). In particular, the heat capacity is shown in figure 1. In [59] a different noncommutative model has been studied without considering the degeneracy of the states.

6.3. Magnetization

The magnetization for the noncommutative Dirac oscillator case is illustrated in figure 8. The figure shows the presence of a fixed point at $M = 0$ for every T. The point where the magnetization changes its sign appears only in the noncommutative case and is a consequence of the term $\partial\xi/\partial X$ in (25), that is a non constant function of X:

$$\frac{\partial \xi_{\mathrm{L,R}}}{\partial X} = \pm 4 \frac{mc^2}{\omega_\theta \hbar} \left[2X - \frac{\hbar\left(\omega_\eta + \omega_\theta\right)}{mc^2} \right] = \pm 4 \sqrt{\frac{m\,c^2}{\hbar\,\omega_\theta} \xi_{\mathrm{L,R}} \pm \frac{(\omega_\eta - \omega_\theta)^2}{\omega_\theta{}^2}} \tag{39}$$

where the plus sign is for the L phase and the minus sign is for the R phase. From the first line of (39), we find that at the point $X_0 = \frac{\hbar(\omega_\eta + \omega_\theta)}{2mc^2}$ the magnetization changes sign. Therefore, the point where the magnetization smoothly vanishes is the midpoint between the two

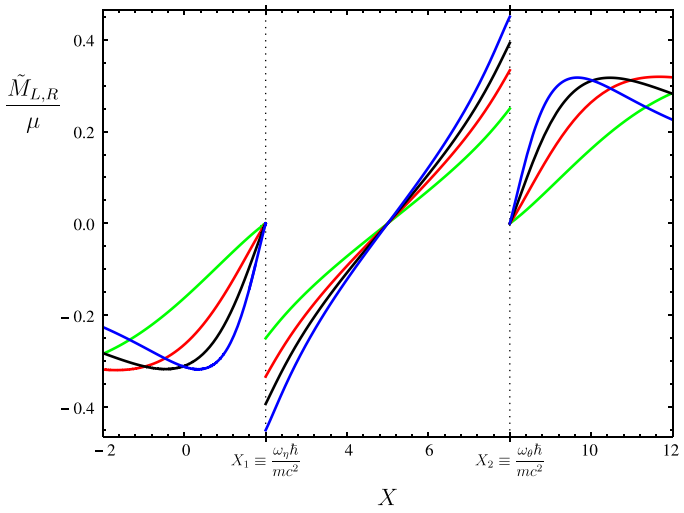

Figure 8. Scaled magnetization in the noncommutative case as function of the scaled effective magnetic energy X, defined in (5), for different values of the rescaled inverse temperature $\tilde{\beta} = 0.5, 0.8, 1.1, 1.5$ respectively green, red, black and blue lines. The parameters are fixed as in figure 7.

critical points. This feature of the noncommutative system is independent of the temperature and was also present in the analysis at $T = 0$ [14]. Near the critical point, we can evaluate the magnetization in $\xi_{\mathrm{L,R}}$ using the second line of (39) and (24) in (25), obtaining:

$$\frac{\partial \xi_{\mathrm{L,R}}}{\partial X} = \pm 4 \left[\left| \frac{(\omega_\eta - \omega_\theta)}{\omega_\theta} \right| \pm \frac{1}{2} \frac{m\,c^2}{\hbar} \frac{\xi_{\mathrm{L,R}}}{|\omega_\eta - \omega_\theta|} + \mathcal{O}(\xi^2) \right], \tag{40}$$

and the other terms in (25) read

$$\frac{1}{\tilde{\beta}} \frac{1}{Z} \frac{\partial Z}{\partial \xi} = \frac{\tilde{\beta}}{4(\tilde{\beta}+1)} (\Theta - 1) + \left[\frac{\tilde{\beta}}{4(\tilde{\beta}+1)} \right]^2 \left[\frac{2}{3} + \tilde{\beta} \left(\Theta - \frac{1}{3} \right) \right] \xi + \mathcal{O}\left(\xi^2\right). \tag{41}$$

Then the discontinuity of the magnetization at the two critical points, for the noncommutative case is

$$\Delta M = \pm \mu \left| \frac{(\omega_\eta - \omega_\theta)}{\omega_\theta} \right| \frac{\tilde{\beta}}{(\tilde{\beta}+1)}, \tag{42}$$

and we can notice that if η, the noncommutative parameter related with the momenta, vanishes then the transitions become independent from θ, the coordinates noncommutative parameter.

7. Conclusions

Over the years, the Dirac oscillator has become a valuable tool for various branches of physics, mostly because it is one of the few relativistic systems whose exact solutions are known. The $(2+1)$-dimensional case, namely when an electron is constrained to live in a plane, manifests

an intrinsic chiral behavior of its states. An external magnetic field interacts at the quantum level with the chirality properties of the system and, if strong enough, it forces an abrupt switch in the electron chirality. This behavior studied at zero temperature, distinguish two phases of the electron at different regimes, and their change is recognized to be a quantum phase transition [12]. Magnetization shows a discontinuity at a finite value of the magnetic field [14]. The quantum nature of this behavior raises the question on how thermal fluctuations interacts with the system and when the thermal disorder destroys these quantum effects. In this paper, we analyze the interplay between these two physical phenomena. In particular, we quantify the discontinuity of the magnetization of the QPT at finite temperature $\Delta M \propto \hbar \left[\frac{1}{k_B T} + O\left(\frac{1}{k_B T}\right)^2\right]$. This discontinuity is a quantum phenomenon that tends to zero for high temperatures. While the critical values of the system are not affected by changes in temperature, we noticed a crucial difference from the system at $T = 0$ studied in [14]: the magnetization at finite temperature has regimes with opposite sign with respect to the single state (zero-temperature) case. This opens to the possibility of a second phase transition at low temperatures, where the statistics of the states becomes quantum and cannot be described by Boltzmann statistics. In figure 6 we report various thermodynamic quantities that can be evaluated once the partition function is provided. The specific heat shows different behaviors at different phases of the system.

The series representations of the partition function proposed in this paper allow to explore the system in diverse regimes: far, close and at the critical points. The representation in terms of the Hurwitz-zeta function fixes some misunderstandings present in the literature regarding which poles play a role in the evaluation of the partition function.

We also generalize our calculations to the Dirac oscillator in noncommutative momenta and coordinates, showing that it manifests a re-entrant quantum phase transition also at finite temperature. Interestingly, there are systems in condensed matter physics that in certain regimes appear to behave as systems living in a noncommutative spacetime [20–23]. This can open the possibility of an analogue noncommutativity. The 'analogue' approach to theoretical models that are too extreme or too weak to be measured directly has already been successfully employed in high-energy physics, and in particular in gravity with the so called analogue gravity [60]. This program is in constant development and already lead to important successes such as the measures of the analogue Hawking radiation [61–64], phenomenon that seemed to be only a theoretical model. It is interesting and challenging to find an analogue system that would allow the experimental measure of the re-entrant phase transition described in this paper, and we leave it for future investigation.

Acknowledgments

The work of AMF was supported by a Swiss Government Excellence Scholarship and is currently supported from ERC Advanced Grant GravBHs-692951 and MEC grant FPA2016-76005-C2-2-P. DM acknowledges L Malagò for discussions and support. PR is thankful to INFN, Sezione di Perugia, and the Department of Physics and Geology of the University of Perugia for support and hospitality.

ORCID iDs

A M Frassino https://orcid.org/0000-0001-9937-486X
O Panella https://orcid.org/0000-0003-4262-894X
P Roy https://orcid.org/0000-0001-9842-2268

Reference

[1] Sachdev S 2011 *Quantum Phase Transitions* 2nd edn (Cambridge: Cambridge University Press)
[2] Moshinsky M and Szczepaniak A 1989 The Dirac oscillator *J. Phys. A: Math. Gen.* **22** L817
[3] Bermudez A, Martin-Delgado M A and Solano E 2007 Exact mapping of the 2+1 Dirac oscillator onto the Jaynes–Cummings model: ion-trap experimental proposal *Phys. Rev.* A **76** 041801
[4] Mandal B P and Rai S K 2012 Noncommutative Dirac oscillator in an external magnetic field *Phys. Lett.* A **376** 2467–70
[5] Luo Z-Y, Wang Q, Xiao L and Jing J 2012 Dirac oscillator in noncommutative phase space and (anti)-Jaynes–Cummings models *Int. J. Theor. Phys.* **51** 2143–51
[6] Hou Y-L, Wang Q, Long Z-W and Jing J 2015 Noncommutative 2+1 dimensional dirac oscillator and quantum phase transition *Ann. Phys.* **354** 10–20
[7] Franco-Villafañe J-A, Sadurni E, Barkhofen S, Kuhl U, Mortessagne F and Seligman T H 2013 First experimental realization of the Dirac oscillator *Phys. Rev. Lett.* **111** 170405
[8] Sadurni E, Seligman T H and Mortessagne F 2010 Playing relativistic billiards beyond graphene *New J. Phys.* **12** 053014
[9] Bermudez A, Martin-Delgado M A and Solano E 2007 Mesoscopic superposition states in relativistic landau levels *Phys. Rev. Lett.* **99** 123602
[10] Bermudez A, Martin-Delgado M A and Luis A 2008 Nonrelativistic limit in the 2 + 1 Dirac oscillator: a Ramsey-interferometry effect *Phys. Rev.* A **77** 033832
[11] Mandal B P and Verma S 2010 Dirac oscillators in presence of external magnetic field *Phys. Lett.* A **374** 1021–3
[12] Bermudez A, Martin-Delgado M A and Luis A 2008 Chirality quantum phase transition in the Dirac oscillator *Phys. Rev.* A **77** 063815
[13] Quimbay C and Strange P 2013 Quantum phase transition in the chirality of the (2+1)-dimensional Dirac oscillator (arXiv:1312.5251 [quant-ph])
[14] Panella O and Roy P 2014 Quantum phase transitions in the noncommutative Dirac Oscillator *Phys. Rev.* A **90** 042111
[15] Panella O and Roy P 2016 Re-entrant phase transitions in non-commutative quantum mechanics *J. Phys.: Conf. Ser.* **670** 012040
[16] Hudson C S 1904 Die gegenseitige löslichkeit von nikotin in wasser *Zeitschrift für Physikalische Chemie* **47** 113–5
[17] Mann R B 2016 The chemistry of black holes *1st Karl Schwarzschild Meeting on Gravitational Physics* ed P Nicolini, M Kaminski, J Mureika and M Bleicher (Cham: Springer) pp 197–205
[18] Altamirano N, Kubiznak D and Mann R B 2013 Reentrant phase transitions in rotating anti–de Sitter black holes *Phys. Rev.* D **88** 101502
[19] Frassino A M, Kubiznak D, Mann R B and Simovic F 2014 Multiple reentrant phase transitions and triple points in Lovelock thermodynamics *J. High Energy Phys.* JHEP09(2014)080
[20] Neupert T, Santos L, Ryu S, Chamon C and Mudry C 2012 Noncommutative geometry for three-dimensional topological insulators *Phys. Rev.* B **86** 035125
[21] Haldane F D M 2011 Geometrical description of the fractional quantum hall effect *Phys. Rev. Lett.* **107** 116801
[22] Parameswaran S A, Roy R and Sondhi S L 2012 Fractional Chern insulators and the W_∞ algebra *Phys. Rev.* B **85** 241308
[23] Bernevig B A and Regnault N 2012 Emergent many-body translational symmetries of Abelian and non-Abelian fractionally filled topological insulators *Phys. Rev.* B **85** 075128
[24] Kubo R, Ichimura H, Usui T and Hashitsume N 1990 *Statistical Mechanics* North-Holland Personal Library 1st edn (Amsterdam: North-Holland)
[25] Banerjee R and Ghosh S 1998 The Chiral oscillator and its applications in quantum theory *J. Phys.* A **31** L603–8
[26] Horta Barreira M M and Wotzasek C 1992 Chiral boson quantum mechanics *Phys. Rev.* D **45** 1410–5
[27] Dunne G V, Jackiw R and Trugenberger C A 1990 Topological (Chern-Simons) quantum mechanics *Phys. Rev.* D **41** 661
[28] Hakim R 2011 *Introduction to Relativistic Statistical Mechanics: Classical and Quantum* (Singapore: World Scientific)
[29] Brevik I H, Herikstad R and Skriudalen S 2007 Entropy bound for the TM electromagnetic field in the half Einstein universe *Int. J. Mod. Phys.* D **16** 1273–84

[30] Dariescu M-A and Dariescu C 2007 Finite temperature analysis of quantum Hall-type behavior of charged bosons *Chaos, Solitons Fractals* **33** 776–81
[31] Boumali A 2015 The one-dimensional thermal properties for the relativistic harmonic oscillators *EJTP* **12** 121–30 (http://www.ejtp.com/articles/ejtpv12i32p121.pdf)
[32] Paris R B and Kaminski D 2001 *Asymptotics and Mellin-Barnes Integrals* Encyclopedia of Mathematics and its Applications 1st edn (Cambridge: Cambridge University Press)
[33] Paris R B 2005 The Stokes phenomenon associated with the Hurwitz zeta function $\zeta(s, a)$ *Proc. R. Soc.* A **461** 297–304
[34] Magnus W, Oberhettinger F and Soni R 2013 *Formulas and Theorems for the Special Functions of Mathematical Physics* (*Grundlehren der mathematischen Wissenschaften*) (Berlin: Springer)
[35] Yoshioka D and Fukuyama H 1992 Orbital magnetism of two-dimensional electrons in confining potentials *J. Phys. Soc. Japan* **61** 2368–81
[36] Andersen J O and Haugset T 1995 Magnetization in (2+1)-dimensional QED at finite temperature and density *Phys. Rev.* D **51** 3073–80
[37] NIST 2017 *Digital Library of Mathematical Functions* (Version 1.0.15) http://dlmf.nist.gov/
[38] Grosse H and Wulkenhaar R 2012 8D-spectral triple on 4D-Moyal space and the vacuum of noncommutative gauge theory *J. Geom. Phys.* **62** 1583–99
[39] Grosse H and Wulkenhaar R 2014 Self-dual noncommutative ϕ^4 -theory in four dimensions is a non-perturbatively solvable and non-trivial quantum field theory *Commun. Math. Phys.* **329** 1069–130
[40] Grosse H, Alexander H and Wulkenhaar R 2020 Solution of the self-dual Φ^4 QFT-model on four-dimensional Moyal space *J. High Energy Phys.* JHEP01(2020)081
[41] Vitale P and Wallet J-C 2013 Noncommutative field theories on R^3_λ: toward UV/IR mixing freedom *J. High Energy Phys.* JHEP04(2013)115
Vitale P and Wallet J-C 2015 Addendum: Noncommutative field theories on R^3_λ: toward UV/IR mixing freedom *J. High Energy Phys.* JHEP03(2015)115
[42] Martinetti P, Vitale P and Wallet J-C 2013 Noncommutative gauge theories on $\mathbb{R}^2_\theta$as matrix models *J. High Energy Phys.* JHEP09(2013)051
[43] Antoine G, Vitale P and Wallet J-C 2014 Quantum gauge theories on noncommutative three-dimensional space *Phys. Rev.* D **90** 045019
[44] Amelino-Camelia G and Arzano M 2002 Coproduct and star product in field theories on Lie algebra noncommutative space-times *Phys. Rev.* D **65** 084044
[45] Agostini A, Amelino-Camelia G and Arzano M 2004 Dirac spinors for doubly special relativity and kappa Minkowski noncommutative space-time *Class. Quantum Grav.* **21** 2179–202
[46] Agostini A, Amelino-Camelia G, Arzano M and D'Andrea F 2006 A cyclic integral on kappa-Minkowski noncommutative space-time *Int. J. Mod. Phys.* A **21** 3133–50
[47] Agostini A, Amelino-Camelia G, Arzano M, Marciano A and Tacchi R A 2007 Generalizing the noether theorem for Hopf-algebra spacetime symmetries *Mod. Phys. Lett.* A **22** 1779–86
[48] Bertolami O, Rosa J G, de Aragao C M L, Castorina P and Zappala D 2005 Noncommutative gravitational quantum well *Phys. Rev.* D **72** 025010
[49] Gamboa J, Loewe M, Mendez F and Rojas J C 2002 Noncommutative quantum mechanics: the two-dimensional central field *Int. J. Mod. Phys.* A **17** 2555–66
[50] Itô D, Mori K and Carriere E 1967 An example of dynamical systems with linear trajectory *Il Nuovo Cimento* A **51** 1119–21
[51] Bellucci S, Nersessian A and Sochichiu C 2001 Two phases of the noncommutative quantum mechanics *Phys. Lett.* B **522** 345–9
[52] Duval C and Horvathy P A 2000 The Peierls substitution and the exotic Galilei group *Phys. Lett.* B **479** 284–90
[53] Gamboa J, Loewe M, Mendez F and Rojas J C 2001 The Landau problem and noncommutative quantum mechanics *Mod. Phys. Lett.* A **16** 2075–8
[54] Gamboa J, Loewe M and Rojas J C 2001 Noncommutative quantum mechanics *Phys. Rev.* D **64** 067901
[55] Horvathy P A, Martina L and Stichel P C 2010 Exotic galilean symmetry and non-commutative mechanics *Symmetry, Integrability Geometry Methods Appl.* **6** 060
[56] Nair V P and Polychronakos A P 2001 Quantum mechanics on the noncommutative plane and sphere *Phys. Lett.* B **505** 267–74
[57] Smailagic A and Spallucci E 2002 Isotropic representation of the noncommutative 2D harmonic oscillator *Phys. Rev.* D **65** 107701
[58] Smailagic A and Spallucci E 2002 Noncommutative 3-D harmonic oscillator *J. Phys. A: Math. Gen.* **35** L363–8

[59] Boumali A and Hassan H 2013 The thermal properties of a two-dimensional dirac oscillator under an external magnetic field *Eur. Phys. J. Plus* **128** 124
[60] Barcelo C, Liberati S and Visser M 2005 Analogue gravity *Living Rev. Relativ.* **8** 12
Barcelo C, Liberati S and Visser M 2011 Analogue gravity *Living Rev. Relativ.* **14** 3
[61] Weinfurtner S, Tedford E W, Penrice M C J, Unruh W G and Lawrence G A 2011 Measurement of stimulated Hawking emission in an analogue system *Phys. Rev. Lett.* **106** 021302
[62] Belgiorno F, Cacciatori S L, Clerici M, Gorini V, Ortenzi G, Rizzi L, Rubino E, Sala V G and Faccio D 2010 Hawking radiation from ultrashort laser pulse filaments *Phys. Rev. Lett.* **105** 203901
[63] Steinhauer J 2014 Observation of self-amplifying Hawking radiation in an analog black hole laser *Nat. Phys.* **10** 864
[64] Steinhauer J 2016 Observation of thermal Hawking radiation and its entanglement in an analogue black hole *Nat. Phys.* **12** 959